Streptococcus pneumoniae evades host cell phagocytosis and limits host mortality through its cell wall anchoring protein PfbA

Running title: PfbA inhibits phagocytosis and limits host responses

Masaya Yamaguchi[a, #], Yujiro Hirose[a], Moe Takemura[a, b], Masayuki Ono[a, c], Tomoko Sumitomo[a], Masanobu Nakata[a], Yutaka Terao[d], Shigetada Kawabata[a]

[a]Department of Oral and Molecular Microbiology, Osaka University Graduate School of Dentistry, Osaka, Japan

[b]Department of Oral and Maxillofacial Surgery II, Osaka University Graduate School of Dentistry, Osaka, Japan

[c]Department of Fixed Prosthodontics, Osaka University Graduate School of Dentistry, Osaka, Japan.

[d]Division of Microbiology and Infectious Diseases, Niigata University Graduate School of Medical and Dental Sciences, Niigata, Japan

17 #Address correspondence to Masaya Yamaguchi, yamaguchi@dent.osaka-u.ac.jp

18

19 Word count: 5255 words

Abstract

Streptococcus pneumoniae is a Gram-positive bacterium belonging to the oral streptococcus species, mitis group. This pathogen is a leading cause of community-acquired pneumonia, which often evades host immunity and causes systemic diseases, such as sepsis and meningitis. Previously, we reported that PfbA is a β-helical cell surface protein contributing to pneumococcal adhesion to and invasion of human epithelial cells in addition to its survival in blood. In the present study, we investigated the role of PfbA in pneumococcal pathogenesis. Phylogenetic analysis indicated that the *pfbA* gene is specific to *S. pneumoniae* within the mitis group. Our *in vitro* assays showed that PfbA inhibits neutrophil phagocytosis, leading to pneumococcal survival. We found that PfbA activates NF-κB through TLR2, but not TLR4. In addition, TLR2/4 inhibitor peptide treatment of neutrophils enhanced the survival of the *S. pneumoniae* Δ*pfbA* strain as compared to a control peptide treatment, whereas the treatment did not affect survival of a wild-type strain. In a mouse pneumonia model, the host mortality and level of TNF-α in bronchoalveolar lavage fluid were comparable between wild-type and Δ*pfbA*-infected mice, while deletion of

pfbA increased the bacterial burden in bronchoalveolar lavage fluid. In a mouse sepsis model, the Δ*pfbA* strain demonstrated significantly increased host mortality and TNF-α levels in plasma, but showed reduced bacterial burden in lung and liver. These results indicate that PfbA may contribute to the success of *S. pneumoniae* species by inhibiting host cell phagocytosis, excess inflammation, and mortality.

Importance

Streptococcus pneumoniae is often isolated from the nasopharynx of healthy children, but the bacterium is also a leading cause of pneumonia, meningitis, and sepsis. In this study, we focused on the role of a cell wall anchoring protein, PfbA, in the pathogenesis of *S. pneumoniae*-related disease. We found that PfbA is a pneumococcus-specific anti-phagocytic factor that functions as a TLR2 ligand, indicating that PfbA may represent a pneumococcal-specific therapeutic target. However, a mouse pneumonia model revealed that PfbA deficiency reduced the bacterial burden, but did not decrease host mortality. Furthermore, in a mouse sepsis model, PfbA deficiency increased host mortality. These results suggest that *S.*

pneumoniae optimizes reproduction by regulating host mortality through PfbA; therefore, PfbA inhibition would not be an effective strategy for combatting pneumococcal infection. Our findings underscore the challenges involved in drug development for a bacterium harboring both commensal and pathogenic states.

Introduction

Streptococcus pneumoniae is Gram-positive bacteria belonging to the mitis group that colonizes the human nasopharynx in approximately 20% of children without causing clinical symptoms (1-3). On the other hand, *S. pneumoniae* is also a leading cause of bacterial pneumonia, meningitis, and sepsis worldwide. The pathogen is estimated to be responsible for the deaths of approximately 1,190,000 people annually from lower respiratory infection (4). Following the introduction of pneumococcal conjugate vaccines, *S. pneumoniae* is still responsible for two thirds of all cases of meningitis (5). In addition, antibiotic selective pressure causes resistant pneumococcal clones to emerge and expand all over the world and the World Health Organization listed *S. pneumoniae* as one of antibiotic-resistant "priority pathogens" (6). Centers for

Disease Control and Prevention data from active bacterial core surveillance for 2009 to 2013 indicated that pneumococcal conjugate vaccines work as a useful tool against antibiotic resistance (7). However, these vaccines also generate selective pressure, and non-vaccine serotypes of *S. pneumoniae* are increasing worldwide (8, 9).

During the process of invasive infection, *S. pneumoniae* needs to evade host immunity and replicate in the host after colonization. In these steps, pneumococcal cell surface proteins work as adhesins and/or anti-phagocytic factors. There are two types of motifs for pneumococcal cell surface localization, a cell wall anchoring motif, LPXTG (10), and choline-binding repeats interacting with pneumococcal phosphorylcholine (11). Choline-binding proteins (CBPs) localize on the pneumococcal cell wall via the phosphorylcholine moiety of teichoic acids, while LPXTG-anchored proteins are covalently attached to the cell wall. Several LPXTG-anchored proteins and CBPs contribute to the adhesion to host epithelial cells through the interaction with host factors (10-13). Some pneumococcal cell surface proteins also contribute to bacterial survival by limiting complement deposition or inhibiting phagocytosis (11, 14-17). On the other hand, the host recognizes *S. pneumoniae* and regulates immune responses

using pattern recognition receptors, including the Toll-like receptors (TLRs), nucleotide oligomerization domain-like receptors, and retinoic acid-inducible gene-I-like receptors (18). In addition, extracellular bacteria are recognized by TLR2 and TLR4 located on the host cell surface. TLR2 recognizes pneumococcal cell wall components and lipoproteins, while TLR4 senses a pore-forming toxin, pneumolysin (18, 19). Generally, both TLR2 and TLR4 agonists induce neutrophil activation and inhibit the apoptosis (20). However, in mouse influenza A virus and *S. pneumoniae* co-infection model, a TLR2 agonist decreased inflammation and reduced bacterial shedding and transmission (21). TLRs play important, but redundant, roles in the host defense and regulating inflammatory responses against pneumococcal infection. Appropriate immune responses contribute to pneumococcal clearance, while excessive inflammation can lead to serious tissue damage.

We previously reported that plasmin- and fibronectin-binding protein A (PfbA) plays a role in fibronectin-dependent adhesion to and invasion of epithelial cells, and that an *S. pneumoniae* PfbA-deficient mutant strain exhibited decreased survival in human blood (22, 23). PfbA is an LPXTG-anchored protein that features a right-handed

parallel β-helix with a groove or cleft, formed by three parallel β-sheets and connecting loops (24, 25). Since the distribution and structural arrangement of the groove residues in the β-helix make it favorable for binding to carbohydrates, PfbA binds to D-galactose, D-mannose, D-glucosamine, D-galactosamine, *N*-acetylneuraminic acid, D-sucrose, and D-raffinose (26). PfbA also binds to human erythrocytes by interacting with *N*-acetylneuraminic acids on the cells (27).

In this study, we investigated the role of PfbA in pneumococcal pathogenesis. Phylogenetic analysis indicated that *pfbA* is specific to *S. pneumoniae* among the mitis group *Streptococcus*. Our *in vitro* analysis revealed that PfbA works as an anti-phagocytic factor and that the protein causes NF-κB activation via TLR2. In addition, Toll-interleukin 1 receptor adaptor protein (TIRAP) inhibition increased the survival rate of the *pfbA* mutant strain after incubation with neutrophils, while the wild-type (WT) strain was not affected. Mouse infection assays suggested that PfbA contributes to pneumococcal survival in at least some organs. However, in a mouse sepsis model, *pfbA* mutant strain-infected mice showed significantly higher mortality

115 and TNF-α levels in blood. Our findings indicate that PfbA is a pneumococcus-specific

116 anti-phagocytic factor and suppresses host excess inflammation.

117

Materials and Methods

Bacterial strains and construction of mutant strain

Streptococcus pneumoniae strains were cultured in Todd-Hewitt broth (BD Biosciences, San Jose, CA, USA) supplemented with 0.2% yeast extract THY medium, BD Biosciences) at 37°C. For selection and maintenance of mutants, spectinomycin (Fujifilm Wako Pure Chemical Corporation, Osaka, Japan) was added to the medium at 120 µg/mL. The *Escherichia coli* strain XL10-Gold (Agilent, Santa Clara, CA, USA) was used as a host for derivatives of plasmid pQE-30. All *E. coli* strains were cultured in Luria-Bertani (LB) broth supplemented with 100 µg/mL carbenicillin (Nacalai Tesque, Kyoto, Japan) at 37°C with agitation.

S. pneumoniae TIGR4 isogenic *pfbA* mutant strains were generated as previously described with minor modifications (22, 28, 29). Briefly, the upstream region of *pfbA*, an *aad9* cassette, the downstream region of *pfbA,* and pGEM-T Easy vector (Promega, Madison, WI, USA) were amplified by PrimeSTAR® MAX DNA Polymerase (TaKaRa Bio, Shiga, Japan) using the specific primers listed in Supplementary Table 1. The DNA fragments were assembled using a GeneArt® Seamless Cloning and Assembly Kit (Thermo Fisher Scientific, Waltham, MA, USA). The constructed plasmid was then

transformed into *E. coli* XL-10 Gold, and the inserted DNA region was amplified by PCR. The products were used to construct mutant strains by double-crossover recombination with the synthesized competence-stimulating peptide-2. The mutation was confirmed by PCR amplification of genomic DNA isolated from the mutant strain.

Cell culture

Human promyelocytic leukemia cells (HL-60, RCB0041) were purchased from RIKEN Cell Bank (Ibaraki, Japan). HL-60 cells were maintained in RPMI 1640 medium (Thermo Fisher Scientific) supplemented with 10% FBS, and were incubated at 37°C in 5% CO_2. HL-60 cells were differentiated into neutrophil-like cells for 5 days in culture media containing 1.2% DMSO (30, 31). Cell differentiation was confirmed by nitro blue tetrazolium reduction assay (30).

Human TLR2/NF-κB/SEAP stably transfected HEK293 cells and human TLR4/MD-2/CD14/NF-κB/SEAP stably transfected HEK293 cells (Novus Biologicals, Centennial, CO, USA, currently sold by InvivoGen, San Diego, CA, USA) were maintained in DMEM with 4.5 g/L glucose, 10% FBS, 4 mM L-glutamine, 1 mM

151 sodium pyruvate, 100 units/mL penicillin, 100 µg/mL streptomycin, 10 µg/mL
152 blasticidin, and 500 µg/mL G418 and DMEM with 4.5 g/L glucose, 10% FBS, 4 mM
153 L-glutamine, 1 mM sodium pyruvate, 100 units/mL penicillin, 100 µg/mL streptomycin,
154 10 µg/mL blasticidin, 2 µg/mL puromycin, 200 µg/mL zeocin, and 500 µg/mL G418,
155 respectively. A secreted alkaline phosphatase reporter assay was performed according to
156 the manufacturer's instructions (Novus Biologicals).
157
158 **Phylogenetic analysis**
159 Phylogenetic analysis was performed as described previously (17, 32, 33), with
160 minor modifications. Briefly, homologues and orthologues of the *pfbA* gene were
161 searched using tBLASTn (34). The sequences were aligned using Phylogears2 (35, 36)
162 and MAFFT v.7.221 with an L-INS-i strategy (37), and ambiguously aligned regions
163 were removed using Jalview (38, 39). The best-fitting codon evolutionary models for
164 phylogenetic analyses were determined using Kakusan4 (40). Bayesian Markov chain
165 Monte Carlo analyses were performed with MrBayes v.3.2.5 (41), and 4×10^6
166 generations were sampled after confirming that the standard deviation of split

167 frequencies was < 0.01. To validate phylogenetic inferences, maximum likelihood
168 phylogenetic analyses were performed with RAxML v.8.1.20 (42). Phylogenetic trees
169 were generated using FigTree v.1.4.2 (43) based on the calculated data.
170
171 **Human neutrophil and monocyte preparation**
172 Human blood was obtained via venipuncture from healthy donors after obtaining
173 informed consent. The protocol was approved by the institutional review boards of
174 Osaka University Graduate School of Dentistry (H26-E43). Human neutrophils and
175 monocytes were prepared using Polymorphprep (Alere Technologies AS, Oslo,
176 Norway), according to the manufacturer's instructions. Human blood was carefully
177 layered on the Polymorphprep solution in centrifugation tubes, which were then
178 centrifuged at 450 × *g* for 30 min in a swing-out rotor at 20°C. Monocyte and neutrophil
179 fractions were transferred into tubes containing ACK buffer (0.15 M NH_4Cl, 0.01 M
180 $KHCO_3$, 0.1 mM EDTA), then centrifuged, washed in phosphate-buffered saline, and
181 resuspended in RPMI 1640 medium.
182

183 **Neutrophil bactericidal assays**

184 The pneumococcal cells grown to the mid-log phase were resuspended in PBS.
185 TIGR4 strains (3-11 × 10^3 CFUs/well) with or without rPfbA (0, 10, or 100 nM) were
186 combined with human neutrophils or neutrophil like-differentiated HL-60 cells (2 x 10^5
187 cells/well), and R6 strains (1.4-2.0 × 10^2 CFUs/well) were combined with human
188 neutrophils (1 × 10^5 cells/well). The mixture was incubated at 37°C in 5% CO_2 for 1, 2,
189 and 3 h. Viable cell counts were determined by plating diluted samples onto TS blood
190 agar. The growth index was calculated as the number of CFUs at the specified time
191 point/number of CFUs in the initial inoculum. Bacterial phagocytosis was blocked by
192 addition of cytochalasin D (20 μM), and pneumococcal killing was blocked by protease
193 inhibitor cocktail set V (Merck, Darmstat, Germany; 500 μM AEBSF, 150 nM
194 Aprotinin, 1 μM E-64, and 1 μM leupeptin hemisulfate, EDTA-free) at 1 h before
195 incubation. To determine whether TLR2 and TLR4 signaling affect pneumococcal
196 survival, 100 μM TIRAP (TLR2 and TLR4) inhibitor peptide or control peptide (Novus
197 Biologicals) were added to neutrophils at 1 h before incubation.
198

199 **Time-lapse microscopic analysis**

200 For time-lapse observations, isolated neutrophils were resuspended in RPMI 1640
201 at 1×10^6 cells/mL. Next, 10 μL of *S. pneumoniae* R6 wild type or Δ*pfbA* strains ($1 \times$
202 10^6 CFUs) was added to 2 mL of the cells, and the mixture was incubated and observed
203 at 37°C. Time-lapse images were captured using an Axio Observer Z1 microscope
204 system (Carl Zeiss, Oberkochen, Germany).

205

206 **Flow cytometric analysis of phagocytes**

207 Recombinant PfbA (rPfbA) or BSA was coated onto 0.5-μm-diameter fluorescent
208 beads (FluoroSphere, Thermo Fisher Scientific), according to the manufacturer's
209 instructions. rPfbA was purified as previously described (22). Isolated neutrophils or
210 monocytes were then resuspended in RPMI 1640 at 1.0×10^7 cells/mL, after which 900
211 μL of RPMI 1640 containing 1 μL of rPfbA-, BSA-, or non-coated fluorescent beads
212 was added to 100 μL of cells, and then the mixtures were rotated at 37°C for 1 h. The
213 cells were washed twice and fixed with 2% glutaraldehyde-RPMI 1640 at 37°C for 1 h,
214 then washed again three times and analyzed with a CyFlow flow cytometer (Sysmex,

215 Hyogo, Japan) using FlowJo software ver. 8.3.2 (BD Biosciences, Franklin Lakes, NJ,
216 USA).
217
218 **TLR2/4 SEAPorter assay**
219 HEK cells expressing TLR2 or TLR4 were stimulated with *S. pneumoniae* and/or
220 rPfbA for 16 h, according to the manufacturer's instructions (Novus Biologicals). To
221 avoid the effect of bacterial replication on this assay, *S. pneumoniae* were pasteurized
222 by incubation at 56°C for 30 min. To perform the assay under the same condition, rPfbA
223 was also incubated at 56°C for 30 min. Lipopolysaccharides from *Escherichia coli*
224 O111:B4 (Sigma-Aldrich Japan Inc., Tokyo, Japan) for the TLR-4 cell line and
225 Pam3CSK4 and Zymozan (Novus Biologicals) for the TLR-2 cell line were used as
226 positive controls under the same conditions. Secreted alkaline phosphatase (SEAP) was
227 analyzed using the SEAPorter Assay (Novus Biologicals) according to the
228 manufacturer's instructions. Quantitative data (ng/mL) were obtained using a standard
229 curve for the SEAP protein.
230

231 **RNA extraction and miRNA array**

232 We performed microRNA array analysis using neutrophil like-differentiated HL60
233 cells incubated with *S. pneumoniae* strains and/or 100 nM rPfbA for 1 h. We compared
234 rPfbA-treated and non-treated cells, wild type and Δ*pfbA*-infected cells, and Δ*pfbA* with
235 and without rPfbA-infected cells. In each cell sample, six replicates were pooled and
236 total RNA including microRNA was isolated from the pooled cells by miRNeasy Mini
237 Kit (Qiagen, Hilden, Germany). Approximately 1000 ng RNA was used for microarray
238 analysis using Affymetrix GeneChip miRNA 4.0 arrays (Affymetrix, Santa Clara, CA,
239 USA) through Filgen Inc. (Nagoya, Japan). Briefly, the quality of total RNA was
240 assessed using a Bioanalyzer 2100 (Agilent). Hybridization was performed using a
241 FlashTag Biotin HSR RNA Labeling Kit, GeneChip Hybridization Oven 645, and
242 GeneChip Fluidics Station 450. The arrays were scanned by Affymetrix GeneChip
243 Scanner 3000 7G. The GeneChip miRNA 4.0 arrays contain 30,424 total mature
244 miRNA probe sets including 2,578 mature human miRNAs, 2,025 pre-miRNA human
245 probes, and 1,196 Human snoRNA and scaRNA probe sets.
246

247 **Mouse infection assays**

248 Mouse infection assays were performed as previously described (17, 33, 44, 45).
249 For the lung infection model, CD-1 mice (Slc:ICR, 8 weeks, female) were infected
250 intratracheally with 4.3-6.7 × 10^6 CFUs of *S. pneumoniae.* For intratracheal infection,
251 the vocal cords were visualized using an operating otoscope (Welch Allyn, NY, USA),
252 and 40 μL of bacteria was placed onto the trachea using a plastic gel loading pipette tip.
253 Mouse survival was monitored twice daily for 14 days. At 24 h after intratracheal
254 infection, bronchoalveolar lavage fluid (BALF) was collected following perfusion with
255 PBS.

256 For the sepsis model, CD-1 mice (Slc:ICR, 8 weeks, female) were infected
257 intravenously with 3.3-6.5 × 10^5 CFUs of *S. pneumoniae* via the tail vein. Mouse
258 survival was monitored twice daily for 14 days. At 24 and 48 h after infection, blood
259 aliquots were collected from mice following induction of general euthanasia. Brain,
260 lung, and liver samples were collected following perfusion with PBS. Brain and lung
261 whole tissues as well as the anterior segment of the liver were resected. Bacterial counts
262 in the blood as well as organ homogenates were determined by separately plating serial

263 dilutions, with organ counts corrected for differences in organ weight. Detection limits
264 were 50 CFUs/organ and 50 CFUs/mL in blood.

265 The concentrations of TNF-α in BALF and plasma were determined using a
266 Duoset® ELISA Kit (R&D Systems, Minneapolis, MN, USA). Mice plasma was
267 obtained by centrifuging the heparinized blood. All mouse experiments were conducted
268 in accordance with animal protocols approved by the Animal Care and Use Committees
269 at Osaka University Graduate School of Dentistry (28-002-0).

270

271 **Statistical analysis**

272 Statistical analysis of *in vitro* and *in vivo* experiments was performed using a
273 nonparametric analysis, Mann-Whitney *U* test, or Kruskal-Wallis test with Dunn's
274 multiple comparisons test. Mouse survival curves were compared using a log-rank test.
275 $p < 0.05$ was considered to indicate a significant difference. The tests were carried out
276 with Graph Pad Prism version 6.0h (GraphPad Software, Inc., San Diego, CA, USA).

277 **Results**

278 **The *pfbA* gene is specific to *S. pneumoniae* among mitis group *Streptococcus***

279 We searched *pfbA*-homologues by tBLASTn and performed phylogenetic analysis

280 (Fig. 1 and Supplementary Fig. 1). The *pfbA* gene homologues were identified in *S.*

281 *pneumoniae*, *Streptococcus pseudopneumoniae*, and *Streptococcus merionis.* Although

282 16S rRNA sequences cannot distinguish mitis group species, the 16S rRNA of

283 *Streptococcus* sp. strain W10853 showed 99.387% identity to that of *S.*

284 *pseudopneumoniae.* Interestingly, *S. pneumoniae*-related species such as *Streptococcus*

285 *mitis* and *Streptococcus oralis* did not contain the homologues, whereas *S. merionis* had

286 a gene of which the query cover and identity were over 50%. *S. merionis* strain

287 NCTC13788 (also known as WUE3771, DSM 19192, and CCUG 54871), isolated from

288 the oropharynges of Mongolian jirds (*Meriones unguiculatus*), contained 16S rRNA that

289 belongs in a cluster distinct from the mitis group (46). This result indicates that the *pfbA*

290 gene is specific to *S. pneumoniae* and *S. pseudopneumoniae* in the mitis group.

291

292 **PfbA contributes to evasion of neutrophil killing**

293 To investigate whether PfbA contributes to evasion of neutrophil killing, we
294 determined pneumococcal survival rates after incubation with human neutrophils. After
295 3 h incubation, the TIGR4 Δ*pfbA* strain showed a significantly decreased bacterial
296 survival rate. In addition, to clarify whether the observed effects were attributed to PfbA,
297 we also performed the assay with rPfbA. In the presence of 100 nM rPfbA, TIGR4
298 Δ*pfbA* strain demonstrated a recovered survival rate nearly equal to that of the wild-type
299 strain (Fig. 2A). In pneumococcal survival assays with neutrophil-like differentiated
300 HL60 cells, TIGR4 strains showed similar results (Fig. 2B). We also performed the
301 assay using the non-encapsulated strain R6 and human neutrophils. The R6 Δ*pfbA* strain
302 showed significantly decreased survival rates as compared to the wild-type strain after
303 incubation for 1, 2, and 3 h (Fig. 2C). As the R6 strain showed this phenotype at earlier
304 time points than the TIGR4 strain, we performed pneumococcal survival assays using
305 R6 strains with inhibitors (Fig. 2D). Neutrophil phagocytic killing of *S. pneumoniae*
306 requires the serine proteases (47). Thus, we used a protein inhibitor cocktail as a
307 positive control of a neutrophil killing inhibitor. While the R6 Δ*pfbA* strain showed
308 significantly decreased survival rates at 1 h after incubation with human fresh

309 neutrophils in the absence of inhibitors, treatment with an actin polymerization inhibitor,
310 cytochalasin D, reduced the differences among the wild-type and Δ*pfbA* strains as well
311 as the protein inhibitor cocktail. These results indicate that PfbA contributes to
312 pneumococcal evasion of neutrophil phagocytosis.
313
314 **PfbA inhibits neutrophil phagocytosis directly**
315 We confirmed the anti-phagocytic activity of PfbA using flow cytometry and
316 PfbA-coated fluorescent beads (Fig. 3A). The fluorescence intensity of neutrophils and
317 monocytes incubated with PfbA-coated beads was substantially lower as compared with
318 cells incubated with non- or BSA-coated beads. These results indicated that neutrophils
319 and monocytes phagocytosed the non- and BSA-coated fluorescent beads, whereas the
320 PfbA-coated fluorescent beads escaped phagocytosis by neutrophils and monocytes.
321 We performed real-time observations for time-lapse analysis of the interaction
322 between *S. pneumoniae* and neutrophils (Fig. 3B). *S. pneumoniae* strain R6 wild-type
323 and Δ*pfbA* strains were separately incubated with fresh human neutrophils in RPMI
324 1640 medium. After coming into contact with neutrophils, the Δ*pfbA* strain was

325 phagocytosed within 1 min, whereas the wild-type strain was not phagocytosed after
326 more than 5 min. Time-lapse analysis also showed the Δ*pfbA* strain engulfed by
327 neutrophil phagosomes. These results suggest that PfbA can directly inhibit
328 phagocytosis.
329
330 **PfbA works as a TLR2 ligand and may inhibit phagocytosis through TLR2**
331 Some lectins of pathogens work as ligand for TLR2 and TLR4 (48). We previously
332 reported that PfbA can interact with glycolipid and glycoprotein fractions of red blood
333 cells, several monosaccharides, D-sucrose, and D-raffinose (26, 27). Hence, to determine
334 whether PfbA works as a TLR ligand, we performed a SEAP assay using HEK-293 cells
335 stably transfected with either TLR2 or TLR4, NF-κB, and SEAP (Fig. 4A). Pam3CSK4
336 and Zymozan were used as positive controls for the TLR2 ligand, while LPS was used
337 for TLR4. The SEAP assay indicated that pasteurized *S. pneumoniae* TIGR4 wild-type
338 cells activated NF-κB via TLR2, whereas Δ*pfbA* cells did not stimulate cells expressing
339 either TLR2 or TLR4. Pasteurized rPfbA also activated NF-κB dose-dependently
340 through TLR2, but not TLR4. In addition, in the presence of pasteurized rPfbA, Δ*pfbA*

341 cells activated the cells expressing TLR2. Thus, PfbA is responsible for pneumococcal
342 NF-κB activation through TLR2.

343 Next, to determine whether TLR signaling suppresses survival of pneumococci
344 incubated with neutrophils, we performed a neutrophil survival assay using a TIRAP
345 inhibitor peptide (Fig. 4B). Data are presented as the ratio calculated by dividing CFUs
346 in the presence of inhibitor peptide by CFUs in the presence of control peptide. TIRAP
347 is an adaptor protein involved in MyD88-dependent TLR2 and TLR4 signaling
348 pathways. Since the TIRAP inhibitor peptide blocks the interaction between TIRAP and
349 TLRs, the peptide works as a TLR2 and TLR4 inhibitor. The inhibitor peptide treatment
350 increased survival rates of the Δ*pfbA* strain, but did not affect wild-type survival rates.
351 These results indicate that PfbA contributes to the evasion of neutrophil phagocytosis,
352 and TIRAP inhibitor treatment did not change survival rates of pneumococci incubated
353 with neutrophils. On the other hand, the *S. pneumoniae* Δ*pfbA* strain is more easily
354 phagocytosed by neutrophils as compared to the wild-type strain, and this phenotype is
355 abolished by TIRAP inhibitor.

Stimulation of the human monocytic cell line THP1 by a TLR ligand, LPS, induces miR-146a/b expression in an NF-κB-dependent fashion, and this induction inhibits innate immune responses (49). In addition, pneumococcal infection of human macrophages induces expression of several microRNAs, including miR-146a, in a TLR-2-dependent manner, which prevents excessive inflammation (50). We performed microRNA array analysis using neutrophil like-differentiated HL60 cells, *S. pneumoniae* strains and rPfbA (Supplementary Fig. 2, Accession number: GSE128341). We compared rPfbA-treated and non-treated cells, wild type and Δ*pfbA*-infected cells, and Δ*pfbA* with and without rPfbA-infected cells. The analysis revealed only one microRNA, hsa-miR-1281, that was commonly downregulated by 2-fold or greater in the presence of PfbA as compared to in its absence (Supplementary Fig. 2, magenta circle). On the other hand, there were no commonly upregulated miRNAs, including miR-146a/b. In addition, the expression of eight microRNAs was commonly changed in wild-type infection and Δ*pfbA* infection with rPfbA as compared to infection with Δ*pfbA* only. Five micro RNAs (hsa-miR-4674, hsa-miR-3613-3p, hsa-miR-4668-5p, hsa-miR-3197, and hsa-miR-6802-5p) were upregulated, while three (hsa-miR-3935,

372 hsa-miR-1281, and hsa-miR-3613-5p) were downregulated. However, the role of these
373 miRNAs in infectious process remains unclear.
374
375 **PfbA deficiency reduces pneumococcal burden in BALF but does not alter host**
376 **survival rate in a mouse pneumonia model**
377 To investigate the role of PfbA in pneumococcal pathogenesis, we infected mice
378 with *S. pneumoniae* strains intratracheally and compared bacterial CFUs and TNF-α
379 levels in BALF from mice 24 h after infection. There were no differences observed in
380 survival time between mice infected with wild type and Δ*pfbA* strains (Fig. 5A).
381 However, recovered CFUs of wild-type bacteria were significantly greater than those of
382 Δ*pfbA* strains in mouse BALF. In addition, the level of TNF-α in BALF was almost the
383 same in wild type and Δ*pfbA* infection (Fig. 5B).
384
385 **PfbA deficiency increases pneumococcal pathogenicity in a mouse sepsis model**
386 We also investigated the role of PfbA in mice following intravenous infection as a
387 model of sepsis. In the infection model, the Δ*pfbA* strain showed significantly higher

388 levels of virulence as compared to the wild-type strain (Fig. 6A). Furthermore, we
389 compared the TNF-α levels in plasma and examined the bacterial burden in blood, brain,
390 lung, and liver samples obtained at 24 and 48 h after intravenous infection (Fig. 6B, 6C
391 and Supplementary Fig. 3). At 24 h after infection, TNF-α ELISA findings showed a
392 significantly greater level in the plasma of *pfbA* mutant strain-infected mice as
393 compared to the wild-type strain-infected mice. The numbers of CFUs of both the
394 wild-type and *pfbA* mutant strains in the blood and brain samples were comparable. On
395 the other hand, in the lung and liver samples, the *pfbA* mutant strain-infected mice
396 showed slightly but significantly reduced numbers of CFUs as compared with the
397 wild-type strain-infected mice. At 48 h after infection, there were no significant
398 differences in TNF-α level and bacterial burden in each organ between the wild-type-
399 and *pfbA* mutant strain-infected mice (Supplementary Fig. 3). Bacteria were not
400 detected in the blood of two of the wild-type strain-infected mice and five of the *pfbA*
401 mutant strain-infected mice. Meanwhile, three of the wild-type strain-infected mice
402 yielded more than 10^6 CFUs/mL, while seven of the wild-type strain-infected mice did.

403 The *pfbA* mutant strain infection caused a polarized bacterial burden in the host at 48 h

404 after infection as compared to wild type infection.

Discussion

In the present study, we found that *pfbA* is a pneumococcal-specific gene that contributes to evasion of neutrophil phagocytosis. We determined that PfbA can activate NF-κB through TLR2. TIRAP inhibition increased the survival rate of Δ*pfbA* strain incubated with neutrophils, while this inhibition did not affect a wild-type strain survival. In a mouse model with lung infection, the bacterial burden of the Δ*pfbA* strain was significantly reduced as compared with that of wild-type strain, but the TNF-α level was comparable between the strains. Overall, there was no significant difference in the survival rates of mice infected with the wild-type *S. pneumoniae* strain- and those infected with the Δ*pfbA* strain. Furthermore, in a mouse model with blood infection, the Δ*pfbA* strain showed a significantly higher TNF-α level than the wild-type strain. These results suggest that PfbA may suppress the host innate immune response by acting as an anti-phagocytic factor interacting with TLR2.

Prior studies have shown that *S. pneumoniae* under selective pressure can adapt to the environment by importing genes from other related streptococci, such as those in the mitis group (51-54). Although *S. mitis* and *S. oralis* are oral commensal bacteria, these

421 species contain various pneumococcal virulence factor homologues. Some mitis group
422 strains harbor several choline-binding proteins including autolysins, pneumolysin,
423 sialidases, and others (11, 55, 56). In this study, we found that *pfbA* homologues were
424 absent among mitis group strains without *S. pneumoniae* for which whole genome
425 sequences were available, whereas the *pfbA* gene is highly conserved among
426 pneumococcal strains. Interestingly, a streptococcal species with clear evolutionary
427 separation from the mitis group, *S. merionis*, contained a *pfbA* orthologue. This result
428 indicates that *pfbA* is a pneumococcal-specific gene and that ancestral *S. pneumoniae*
429 likely obtained the gene by horizontal gene transfer from non-mitis group streptococcal
430 species.

431 Although lipoproteins are major TLR2 ligands as well as peptidoglycans in *S.*
432 *pneumoniae* (19), we found that rPfbA can activate NF-κB solely in HEK293 cells
433 expressing TLR2, but not those expressing TLR4. Since *E. coli* does not have the
434 capacity to glycosylate proteins (57), rPfbA-mediated TLR2 activation would be
435 independent of pneumococcal glycosylation. Plant and pathogen lectins can induce
436 NF-κB activation through binding to TLR2 *N*-glycans, while a classical ligand such as

437 Pam3CSK4 can activate NF-κB glycan-independently (48). TLR2 has four *N*-glycans
438 whose structures still remain unknown, and the *N*-glycans are critical for the lectins to
439 induce TLR2-mediated activation (48). PfbA binds to various carbohydrates via the
440 groove residues in the β-helix (26, 27). There is a possibility that PfbA induces TLR2
441 signaling by binding to TLR2 *N*-glycans.

442 Human macrophages challenged with *S. pneumoniae* induce a negative feedback
443 loop, preventing excessive inflammation via miR-146a and potentially other miRNAs
444 on the TLR2-MyD88 axis (50). On the other hand, pneumococcal endopeptidase O
445 enhances macrophage phagocytosis in a TLR2- and miR-155-dependent manner (58).
446 Furthermore, miR-9 is induced by TLR agonists and functions in feedback control of
447 the NF-κB-dependent responses in human monocytes and neutrophils (59). These
448 studies indicate that host phagocytes are regulated by a complex combination of pattern
449 recognition receptor signaling and miRNA induction. We predicted that PfbA
450 suppresses phagocytosis via the induction of miRNAs in a TLR2 dependent fashion.
451 However, an miRNA array showed that the levels of the involved miRNAs were not
452 changed over 2-fold in the presence or absence of PfbA. One possible hypothesis is that

453 PfbA induces different miRNA responses from classical TLR ligands via
454 glycan-dependent recognition. Although PfbA can downregulate miR-1281 in
455 differentiated HL-60 cells, the role of miR-1281 in phagocytes remains unclear. Further
456 comprehensive studies are required to investigate the role of miRNAs in host innate
457 immunity.

458 Unexpectedly, our mouse pneumonia and sepsis models indicated that *pfbA*
459 deficiency reduces pneumococcal survival in the host, but does not decrease or
460 increases host mortality. We previously reported that PfbA works as an adhesin and
461 invasin of host epithelial cells (22). The reduction of bacterial burden in host organs can
462 be explained by the synergy of adhesive and anti-phagocytic abilities. On the other hand,
463 the *S. pneumoniae* Δ*pfbA* strain showed equivalent or greater induction of inflammatory
464 cytokines as compared with the wild-type strain. Generally, a deficiency of TLR ligands
465 would suppress inflammatory responses. However, a deficiency of PfbA would cause
466 more efficient bacterial uptake by phagocytes and promote inflammatory responses. In
467 addition, there is a possibility that the negative feedback loop induced by PfbA is lost
468 and causes excess inflammation. High mortality does not mean bacterial success, as

host death leads to the limitation of bacterial reproduction. PfbA may be beneficial for pneumococcal species by increasing the bacterial reproductive number through suppression of host cell phagocytosis and host mortality. PfbA showed high specificity for and conservation in *S. pneumoniae* species. The assumed negative feedback loop may not be as significant in non-pathogenic mitis group *Streptococcus*.

In single toxin-induced infectious diseases such as diphtheria and tetanus, highly safe and protective vaccines are established. On the other hand, in multiple factor-induced diseases such as those caused by *S. pneumoniae, S. pyogenes*, and so on, there are either no approved vaccines or existing vaccines still need optimization. Our study indicates that PfbA is a pneumococcal specific cell surface protein, which contributes to evasion from phagocytosis. Therefore, PfbA would not be suitable as a vaccine antigen, since the protein suppresses pneumococcal virulence in a mouse sepsis model. Further investigation of the intricate balance between host immunity and pathogenesis is required to establish the basis for drug and vaccine design.

Acknowledgements

This study was supported by the Japanese Society for the Promotion of Science (JSPS), KAKENHI [grant numbers 26861546, 15H05012, 16H05847, 16K15787, 17H05103, 17K11666, and 18K19643], the SECOM Science and Technology Foundation, Takeda Science Foundation, GSK Japan Research Grant, Asahi Glass Foundation, Kurata Memorial Hitachi Science and Technology Foundation, Kobayashi International Scholarship Foundation, and the Naito Foundation.

Author contributions

M.Y. and S.K. designed the study. M.Y. performed bioinformatics analyses. M.Y., Y.H., M.T., and M.O. performed the experiments. M.Y., T.S., M.N., Y.T., and S.K. contributed to the setup of the experiments. M.Y. wrote the manuscript. Y.H., M.T., M.O., T.S., M.N., Y.T., and S.K. contributed to the writing of the manuscript.

Conflict of interest

The authors declare that they have no competing interests.

References

1. Kawamura Y, Hou XG, Sultana F, Miura H, Ezaki T. 1995. Determination of 16S rRNA sequences of *Streptococcus mitis* and *Streptococcus gordonii* and phylogenetic relationships among members of the genus *Streptococcus*. Int J Syst Evol Micrbiol 45:406-8.
2. Richards VP, Palmer SR, Pavinski Bitar PD, Qin X, Weinstock GM, Highlander SK, Town CD, Burne RA, Stanhope MJ. 2014. Phylogenomics and the dynamic genome evolution of the genus *Streptococcus*. Genome Biol Evol 6:741-53.
3. Bogaert D, van Belkum A, Sluijter M, Luijendijk A, de Groot R, Rumke HC, Verbrugh HA, Hermans PW. 2004. Colonisation by *Streptococcus pneumoniae* and *Staphylococcus aureus* in healthy children. Lancet 363:1871-2.
4. Collaborators GL. 2017. Estimates of the global, regional, and national morbidity, mortality, and aetiologies of lower respiratory tract infections in 195 countries: a systematic analysis for the Global Burden of Disease Study 2015. Lancet Infect Dis 17:1133-1161.
5. McIntyre PB, O'Brien KL, Greenwood B, van de Beek D. 2012. Effect of vaccines on bacterial meningitis worldwide. Lancet 380:1703-11.
6. WHO. 2017. WHO priority pathogens list for R&D of new antibiotics. http://www.who.int/mediacentre/news/releases/2017/bacteria-antibiotics-needed/en/. Accessed
7. Kim L, McGee L, Tomczyk S, Beall B. 2016. Biological and Epidemiological Features of Antibiotic-Resistant *Streptococcus pneumoniae* in Pre- and Post-Conjugate Vaccine Eras: a United States Perspective. Clin Microbiol Rev 29:525-52.
8. Golubchik T, Brueggemann AB, Street T, Gertz RE, Jr., Spencer CC, Ho T, Giannoulatou E, Link-Gelles R, Harding RM, Beall B, Peto TE, Moore MR, Donnelly P, Crook DW, Bowden R. 2012. Pneumococcal genome sequencing tracks a vaccine escape variant formed through a multi-fragment recombination event. Nat Genet 44:352-5.
9. Flasche S, Van Hoek AJ, Sheasby E, Waight P, Andrews N, Sheppard C, George R, Miller E. 2011. Effect of pneumococcal conjugate vaccination on serotype-specific carriage and invasive disease in England: a cross-sectional

532 study. PLoS Med 8:e1001017.
533 10. Lofling J, Vimberg V, Battig P, Henriques-Normark B. 2011. Cellular
534 interactions by LPxTG-anchored pneumococcal adhesins and their streptococcal
535 homologues. Cell Microbiol 13:186-97.
536 11. Hakenbeck R, Madhour A, Denapaite D, Bruckner R. 2009. Versatility of
537 choline metabolism and choline-binding proteins in *Streptococcus pneumoniae*
538 and commensal streptococci. FEMS Microbiol Rev 33:572-86.
539 12. Mitchell AM, Mitchell TJ. 2010. *Streptococcus pneumoniae*: virulence factors
540 and variation. Clin Microbiol Infect 16:411-8.
541 13. Weiser JN, Ferreira DM, Paton JC. 2018. *Streptococcus pneumoniae*:
542 transmission, colonization and invasion. Nat Rev Microbiol 16:355-367.
543 14. Ren B, McCrory MA, Pass C, Bullard DC, Ballantyne CM, Xu Y, Briles DE,
544 Szalai AJ. 2004. The virulence function of *Streptococcus pneumoniae* surface
545 protein A involves inhibition of complement activation and impairment of
546 complement receptor-mediated protection. J Immunol 173:7506-12.
547 15. Dave S, Carmicle S, Hammerschmidt S, Pangburn MK, McDaniel LS. 2004.
548 Dual roles of PspC, a surface protein of *Streptococcus pneumoniae*, in binding
549 human secretory IgA and factor H. J Immunol 173:471-7.
550 16. Gutierrez-Fernandez J, Saleh M, Alcorlo M, Gomez-Mejia A, Pantoja-Uceda D,
551 Trevino MA, Voss F, Abdullah MR, Galan-Bartual S, Seinen J, Sanchez-Murcia
552 PA, Gago F, Bruix M, Hammerschmidt S, Hermoso JA. 2016. Modular
553 Architecture and Unique Teichoic Acid Recognition Features of
554 Choline-Binding Protein L (CbpL) Contributing to Pneumococcal Pathogenesis.
555 Sci Rep 6:38094.
556 17. Yamaguchi M, Goto K, Hirose Y, Yamaguchi Y, Sumitomo T, Nakata M, Nakano
557 K, Kawabata S. 2019. Identification of evolutionarily conserved virulence factor
558 by selective pressure analysis of *Streptococcus pneumoniae*. Commun Biol 2:96.
559 18. Koppe U, Suttorp N, Opitz B. 2012. Recognition of *Streptococcus pneumoniae*
560 by the innate immune system. Cell Microbiol 14:460-6.
561 19. Tomlinson G, Chimalapati S, Pollard T, Lapp T, Cohen J, Camberlein E,
562 Stafford S, Periselneris J, Aldridge C, Vollmer W, Picard C, Casanova JL,
563 Noursadeghi M, Brown J. 2014. TLR-mediated inflammatory responses to
564 *Streptococcus pneumoniae* are highly dependent on surface expression of

565 bacterial lipoproteins. J Immunol 193:3736-45.
566 20. Sabroe I, Dower SK, Whyte MK. 2005. The role of Toll-like receptors in the
567 regulation of neutrophil migration, activation, and apoptosis. Clin Infect Dis 41
568 Suppl 7:S421-6.
569 21. Richard AL, Siegel SJ, Erikson J, Weiser JN. 2014. TLR2 signaling decreases
570 transmission of Streptococcus pneumoniae by limiting bacterial shedding in an
571 infant mouse Influenza A co-infection model. PLoS Pathog 10:e1004339.
572 22. Yamaguchi M, Terao Y, Mori Y, Hamada S, Kawabata S. 2008. PfbA, a novel
573 plasmin- and fibronectin-binding protein of *Streptococcus pneumoniae*,
574 contributes to fibronectin-dependent adhesion and antiphagocytosis. J Biol
575 Chem 283:36272-9.
576 23. Yamaguchi M. 2018. Synergistic findings from microbiological and evolutional
577 analyses of virulence factors among pathogenic streptococcal species. Journal of
578 Oral Biosciences 60:36-40.
579 24. Suits MD, Boraston AB. 2013. Structure of the *Streptococcus pneumoniae*
580 surface protein and adhesin PfbA. PLoS One 8:e67190.
581 25. Beulin DS, Yamaguchi M, Kawabata S, Ponnuraj K. 2014. Crystal structure of
582 PfbA, a surface adhesin of *Streptococcus pneumoniae*, provides hints into its
583 interaction with fibronectin. Int J Biol Macromol 64:168-73.
584 26. Beulin DSJ, Radhakrishnan D, Suresh SC, Sadasivan C, Yamaguchi M,
585 Kawabata S, Ponnuraj K. 2017. *Streptococcus pneumoniae* surface protein PfbA
586 is a versatile multidomain and multiligand-binding adhesin employing different
587 binding mechanisms. FEBS J 284:3404-3421.
588 27. Radhakrishnan D, Yamaguchi M, Kawabata S, Ponnuraj K. 2018. *Streptococcus*
589 *pneumoniae* surface adhesin PfbA and its interaction with erythrocytes and
590 hemoglobin. Int J Biol Macromol 120:135-143.
591 28. Mori Y, Yamaguchi M, Terao Y, Hamada S, Ooshima T, Kawabata S. 2012.
592 α-Enolase of *Streptococcus pneumoniae* induces formation of neutrophil
593 extracellular traps. J Biol Chem 287:10472-81.
594 29. Bricker AL, Camilli A. 1999. Transformation of a type 4 encapsulated strain of
595 *Streptococcus pneumoniae*. FEMS Microbiol Lett 172:131-5.
596 30. Collins SJ, Ruscetti FW, Gallagher RE, Gallo RC. 1979. Normal functional
597 characteristics of cultured human promyelocytic leukemia cells (HL-60) after

598 induction of differentiation by dimethylsulfoxide. J Exp Med 149:969-74.
599 31. Wen X, Jin T, Xu X. 2016. Imaging G Protein-coupled Receptor-mediated
600 Chemotaxis and its Signaling Events in Neutrophil-like HL60 Cells. J Vis Exp
601 doi:10.3791/54511.
602 32. Yamaguchi M, Hirose Y, Nakata M, Uchiyama S, Yamaguchi Y, Goto K,
603 Sumitomo T, Lewis AL, Kawabata S, Nizet V. 2016. Evolutionary inactivation
604 of a sialidase in group B *Streptococcus*. Sci Rep 6:28852.
605 33. Yamaguchi M, Nakata M, Sumioka R, Hirose Y, Wada S, Akeda Y, Sumitomo T,
606 Kawabata S. 2017. Zinc metalloproteinase ZmpC suppresses experimental
607 pneumococcal meningitis by inhibiting bacterial invasion of central nervous
608 systems. Virulence 8:1516-1524.
609 34. Gertz EM, Yu YK, Agarwala R, Schaffer AA, Altschul SF. 2006.
610 Composition-based statistics and translated nucleotide searches: improving the
611 TBLASTN module of BLAST. BMC Biol 4:41.
612 35. Tanabe AS. 2008. Phylogears2 ver. 2.0. http://www.fifthdimension.jp/.
613 Accessed
614 36. Venditti C, Meade A, Pagel M. 2006. Detecting the node-density artifact in
615 phylogeny reconstruction. Syst Biol 55:637-43.
616 37. Katoh K, Standley DM. 2013. MAFFT multiple sequence alignment software
617 version 7: improvements in performance and usability. Mol Biol Evol
618 30:772-80.
619 38. Waterhouse AM, Procter JB, Martin DM, Clamp M, Barton GJ. 2009. Jalview
620 Version 2--a multiple sequence alignment editor and analysis workbench.
621 Bioinformatics 25:1189-91.
622 39. Talavera G, Castresana J. 2007. Improvement of phylogenies after removing
623 divergent and ambiguously aligned blocks from protein sequence alignments.
624 Syst Biol 56:564-77.
625 40. Tanabe AS. 2011. Kakusan4 and Aminosan: two programs for comparing
626 nonpartitioned, proportional and separate models for combined molecular
627 phylogenetic analyses of multilocus sequence data. Mol Ecol Resour 11:914-21.
628 41. Ronquist F, Teslenko M, van der Mark P, Ayres DL, Darling A, Hohna S, Larget
629 B, Liu L, Suchard MA, Huelsenbeck JP. 2012. MrBayes 3.2: efficient Bayesian
630 phylogenetic inference and model choice across a large model space. Syst Biol

631 61:539-42.
632 42. Stamatakis A. 2014. RAxML version 8: a tool for phylogenetic analysis and
633 post-analysis of large phylogenies. Bioinformatics 30:1312-3.
634 43. Rambaut A. 2014. FigTree ver.1.4.2.
635 http://tree.bio.ed.ac.uk/software/figtree/. Accessed
636 44. Okerblom JJ, Schwarz F, Olson J, Fletes W, Ali SR, Martin PT, Glass CK, Nizet
637 V, Varki A. 2017. Loss of CMAH during Human Evolution Primed the
638 Monocyte-Macrophage Lineage toward a More Inflammatory and Phagocytic
639 State. J Immunol 198:2366-2373.
640 45. Hirose Y, Yamaguchi M, Goto K, Sumitomo T, Nakata M, Kawabata S. 2018.
641 Competence-induced protein Ccs4 facilitates pneumococcal invasion into brain
642 tissue and virulence in meningitis. Virulence 9:1576-1587.
643 46. Tappe D, Pukall R, Schumann P, Gronow S, Spiliotis M, Claus H, Brehm K,
644 Vogel U. 2009. *Streptococcus merionis* sp. nov., isolated from *Mongolian jirds*
645 (Meriones unguiculatus). Int J Syst Evol Microbiol 59:766-70.
646 47. Standish AJ, Weiser JN. 2009. Human neutrophils kill *Streptococcus*
647 *pneumoniae* via serine proteases. J Immunol 183:2602-9.
648 48. Ricci-Azevedo R, Roque-Barreira MC, Gay NJ. 2017. Targeting and
649 Recognition of Toll-Like Receptors by Plant and Pathogen Lectins. Front
650 Immunol 8:1820.
651 49. Taganov KD, Boldin MP, Chang KJ, Baltimore D. 2006. NF-κB-dependent
652 induction of microRNA miR-146, an inhibitor targeted to signaling proteins of
653 innate immune responses. Proc Natl Acad Sci U S A 103:12481-6.
654 50. Griss K, Bertrams W, Sittka-Stark A, Seidel K, Stielow C, Hippenstiel S, Suttorp
655 N, Eberhardt M, Wilhelm J, Vera J, Schmeck B. 2016. MicroRNAs Constitute a
656 Negative Feedback Loop in *Streptococcus pneumoniae*-Induced Macrophage
657 Activation. J Infect Dis 214:288-99.
658 51. Bek-Thomsen M, Poulsen K, Kilian M. 2012. Occurrence and evolution of the
659 paralogous zinc metalloproteases IgA1 protease, ZmpB, ZmpC, and ZmpD in
660 *Streptococcus pneumoniae* and related commensal species. MBio 3: e00303-12.
661 52. Kilian M, Riley DR, Jensen A, Bruggemann H, Tettelin H. 2014. Parallel
662 evolution of *Streptococcus pneumoniae* and S*treptococcus mitis* to pathogenic
663 and mutualistic lifestyles. MBio 5:e01490-14.

664 53. Jensen A, Valdorsson O, Frimodt-Moller N, Hollingshead S, Kilian M. 2015.
665 Commensal streptococci serve as a reservoir for β-lactam resistance genes in
666 *Streptococcus pneumoniae*. Antimicrob Agents Chemother 59:3529-40.
667 54. Skov Sorensen UB, Yao K, Yang Y, Tettelin H, Kilian M. 2016. Capsular
668 Polysaccharide Expression in Commensal *Streptococcus* Species: Genetic and
669 Antigenic Similarities to *Streptococcus pneumoniae*. MBio 7:e01844-16.
670 55. Kilian M, Poulsen K, Blomqvist T, Havarstein LS, Bek-Thomsen M, Tettelin H,
671 Sorensen UB. 2008. Evolution of *Streptococcus pneumoniae* and its close
672 commensal relatives. PLoS One 3:e2683.
673 56. Johnston C, Hinds J, Smith A, van der Linden M, Van Eldere J, Mitchell TJ.
674 2010. Detection of large numbers of pneumococcal virulence genes in
675 streptococci of the mitis group. J Clin Microbiol 48:2762-9.
676 57. Clausen H, Wandall HH, Steentoft C, Stanley P, Schnaar RL. 2015.
677 Glycosylation Engineering, p 713-728. *In* Varki A, Cummings RD, Esko JD,
678 Stanley P, Hart GW, Aebi M, Darvill AG, Kinoshita T, Packer NH, Prestegard
679 JH, Schnaar RL, Seeberger PH (ed), Essentials of Glycobiology, 3rd edition
680 doi:10.1101/glycobiology.3e.056. Cold Spring Harbor Laboratory Press, New
681 York.
682 58. Yao H, Zhang H, Lan K, Wang H, Su Y, Li D, Song Z, Cui F, Yin Y, Zhang X.
683 2017. Purified *Streptococcus pneumoniae* Endopeptidase O (PepO) Enhances
684 Particle Uptake by Macrophages in a Toll-Like Receptor 2- and
685 miR-155-Dependent Manner. Infect Immun 85.
686 59. Bazzoni F, Rossato M, Fabbri M, Gaudiosi D, Mirolo M, Mori L, Tamassia N,
687 Mantovani A, Cassatella MA, Locati M. 2009. Induction and regulatory function
688 of miR-9 in human monocytes and neutrophils exposed to proinflammatory
689 signals. Proc Natl Acad Sci U S A 106:5282-7.

690

691

692 **Figure Legends**

693 **Figure 1. Bayesian phylogenetic analysis of the *pfbA* gene.**

694 The codon-based Bayesian phylogenetic relationship was calculated using the MrBayes
695 program. Strains with identical sequences are listed on the same branch. The percentage
696 of posterior probabilities is shown near the nodes. The scale bar indicates nucleotide
697 substitutions per site.

698

699 **Figure 2. PfbA contributes to pneumococcal survival after incubation with**
700 **neutrophils. A.** Growth of TIGR4 strains incubated with human fresh neutrophils. **B.**
701 Growth of TIGR4 strains incubated with neutrophil-like differentiated HL-60 cells.
702 Bacterial cells were incubated with human neutrophils or differentiated HL-60 cells in
703 the presence or absence of rPfbA for 1, 2, and 3 h at 37°C in a 5% CO_2 atmosphere.
704 Next, the mixture was serially diluted and plated on TS blood agar. Following
705 incubation, the number of CFUs was determined. Growth index was calculated by
706 dividing CFUs after incubation by CFUs of the original inoculum. **C.** Growth of R6
707 strains incubated with human fresh neutrophils. *S. pneumoniae* strains were added to

708 human neutrophils without serum and gently mixed for 1, 2, or 3 h at 37°C. Next, the
709 mixtures were serially diluted and plated on TS blood agar. After incubation, the
710 number of CFUs was determined. **D.** Growth of R6 strains incubated with human fresh
711 neutrophils in the presence of inhibitors. *S. pneumoniae* strains were added to human
712 neutrophils with or without cytochalasin D, or protease inhibitor cocktail in the absence
713 of serum, then gently mixed for 1 h at 37°C. The percent bacterial survival was
714 calculated based on viable counts relative to the wild-type strain. These data are
715 presented as the mean values of six samples, with S.E. values represented by vertical
716 lines. Differences between several groups were analyzed using a Kruskal-Wallis test
717 followed by Dunn's multiple comparisons test (A, B). The Mann-Whitney's U test was
718 used to compare differences between two independent groups (C, D). Three
719 experiments were performed, with data from a representative experiment is shown.
720
721 **Figure 3. PfbA suppresses host cell phagocytosis. A.** Uptake of fluorescent
722 PfbA-coated beads by neutrophils and monocytes. Human neutrophils and monocytes
723 were separately incubated with PfbA-, BSA-, or non-coated fluorescent beads for 1 h at

724 37°C. Phagocytic activities were analyzed using flow cytometry. Data are presented as
725 histograms. The value shown for the percent of maximum was determined by dividing
726 the number of cells in each bin by the number of cells in the bin that contained the
727 largest number of cells. The bin is shown as a numerical range for the parameter on the
728 X-axis. **B.** Time-lapse analysis of the interaction between *S. pneumoniae* and
729 neutrophils. *S. pneumoniae* wild-type and Δ*pfbA* strains were incubated with neutrophils.
730 The elapsed times from contact with neutrophils are shown in the upper part of the
731 figures. Arrows indicate when *S. pneumoniae* cells contacted neutrophils. Arrowheads
732 indicate *S. pneumoniae* engulfed by a neutrophil phagosome.
733
734 **Figure 4. PfbA activates NF-κB via TLR2, and TLR2/4 inhibitor enhances Δ*pfbA***
735 **strain survival. A.** Secreted alkaline phosphatase (SEAP) porter assay using
736 TLR2/NF-κB/ SEAPorter or TLR4/MD-2/CD14/NF-κB SEAPorter HEK293 cell lines.
737 The cells were plated in 24-well plates at 5×10^5 cells/well. After 24 h, cells were
738 stimulated with various amount of rPfbA, pasteurized *S. pneumoniae* (~5×10^6 CFU), 1
739 μg/mL Pam3CSK4, 10 μg/mL Zymozan, or 25 ng/mL LPS for 24 h. SEAP was

740 analyzed using the SEAPorter Assay Kit. Data are presented as the mean of six wells.
741 SE values are represented by vertical lines. Differences in pneumococcal infection
742 group and rPfbA addition group were analyzed using a Kruskal-Wallis test followed by
743 Dunn's multiple comparisons test, respectively. **B.** TLR2/4 inhibitor peptide enhances
744 survival of the TIGR4 Δ*pfbA* strain incubated with human neutrophils. *S. pneumoniae*
745 TIGR4 wild type strain or Δ*pfbA* strain bacteria were incubated with human neutrophils
746 in the presence of TLR2/4 inhibitor peptide or control peptide. After 1, 2, and 3 h, the
747 mixture was serially diluted and plated on TS blood agar. Following incubation, the
748 number of CFUs was determined. The CFU ratio was calculated by dividing CFUs in
749 the presence of inhibitor peptide by CFUs in the presence of control peptide. Data are
750 presented as the mean of six wells. S.E. values are represented by vertical lines.
751 Differences between groups were analyzed using Mann-Whitney's U test.
752
753
754 **Figure 5. In a mouse pneumonia model, deficiency of *pfbA* decreases pneumococcal**
755 **burden in the lung but does not affect host mortality. A.** CD-1 mice were infected

intratracheally with the *S. pneumoniae* TIGR4 wild-type or Δ*pfbA* strain (3-18 × 10^6 CFUs). Mice survival was recorded for 14 days. The differences between groups were analyzed using a log-rank test. **B.** Bacterial CFUs and TNF-α in BALF collected from CD-1 mice after intratracheal infection with *S. pneumoniae*. CD-1 mice were infected intratracheally with the *S. pneumoniae* TIGR4 wild type or Δ*pfbA* strain (4-7 × 10^6 CFUs). BALF was collected at 24 h after pneumococcal infection, and bacterial CFUs and TNF-α levels in the BALF were determined. S.E. values are represented by vertical lines. Statistical differences between groups were analyzed using Mann-Whitney's U test. The data obtained from three independent experiments were pooled.

Figure 6. In a mouse sepsis model, the deficiency of *pfbA* increases the virulence and TNF-α level in blood but decreases the bacterial burden in the lung and liver. CD-1 mice were infected intravenously with the *S. pneumoniae* TIGR4 wild type or Δ*pfbA* strain (3-6 × 10^6 CFUs). **A.** Mouse survival was monitored for 14 days. Statistical differences between groups were analyzed using a log-rank test. **B.** CD-1 mice were infected intravenously with the *S. pneumoniae* TIGR4 wild type or Δ*pfbA*

772 strain (6-9 × 10^6 CFUs). Plasma samples were collected from these mice at 24 h after

773 infection. Values are presented as the mean of 16 or 18 samples. Vertical lines represent

774 the mean ± S.E. Statistical differences between groups were analyzed using

775 Mann-Whitney's U test. **C.** The bacterial burden in the blood, brain, lung, and liver

776 were assessed after 24 h of infection. S.E. values are represented by vertical lines. All

777 mice were perfused with PBS after blood collection, organ samples were collected.

778 Statistical differences between groups were analyzed using Mann-Whitney's U test. The

779 mouse survival data were obtained from three independent experiments, and the TNF-α

780 level and bacterial burden values obtained from two independent experiments were

781 pooled.

782

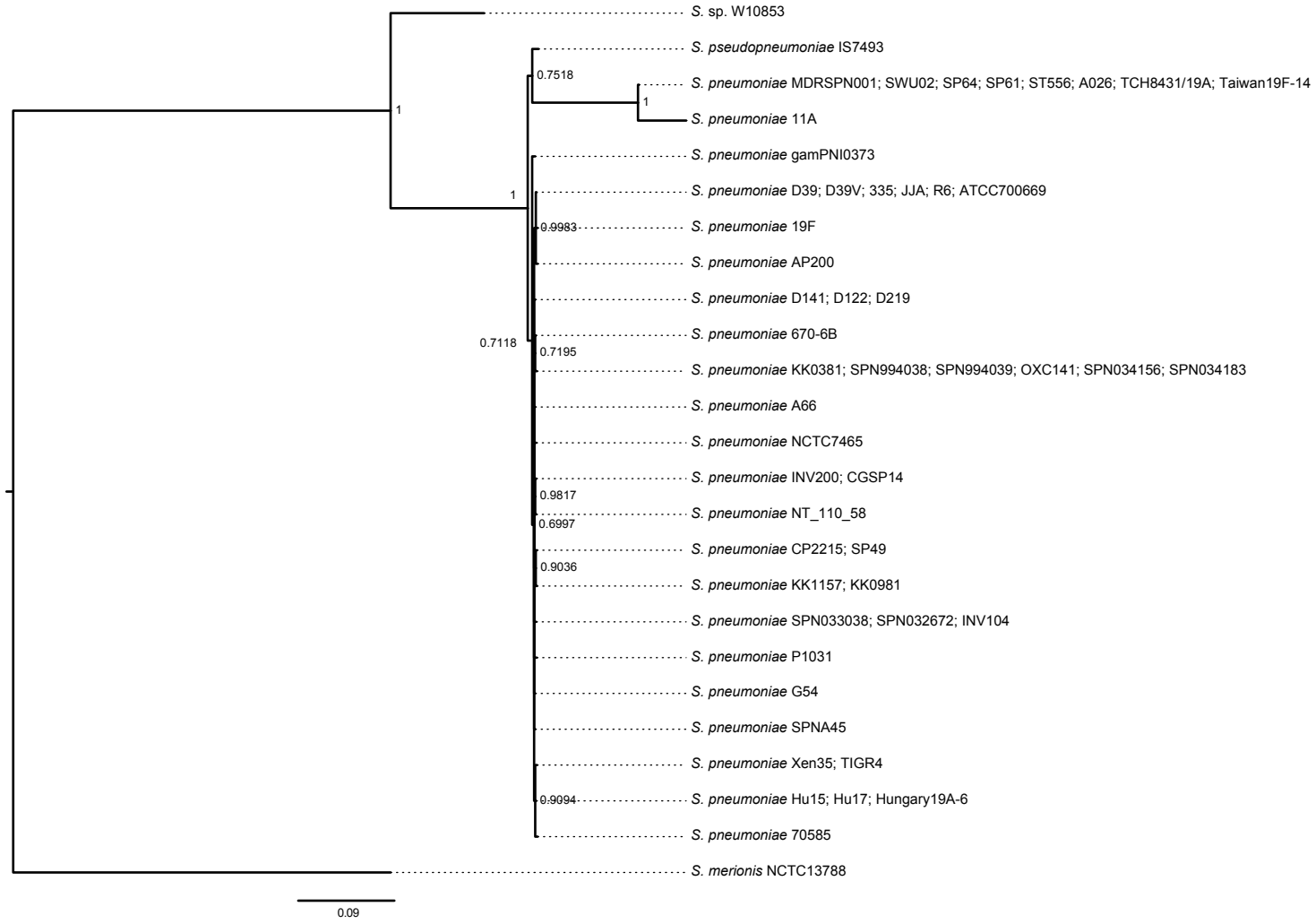

Figure 1. Yamaguchi *et al.*

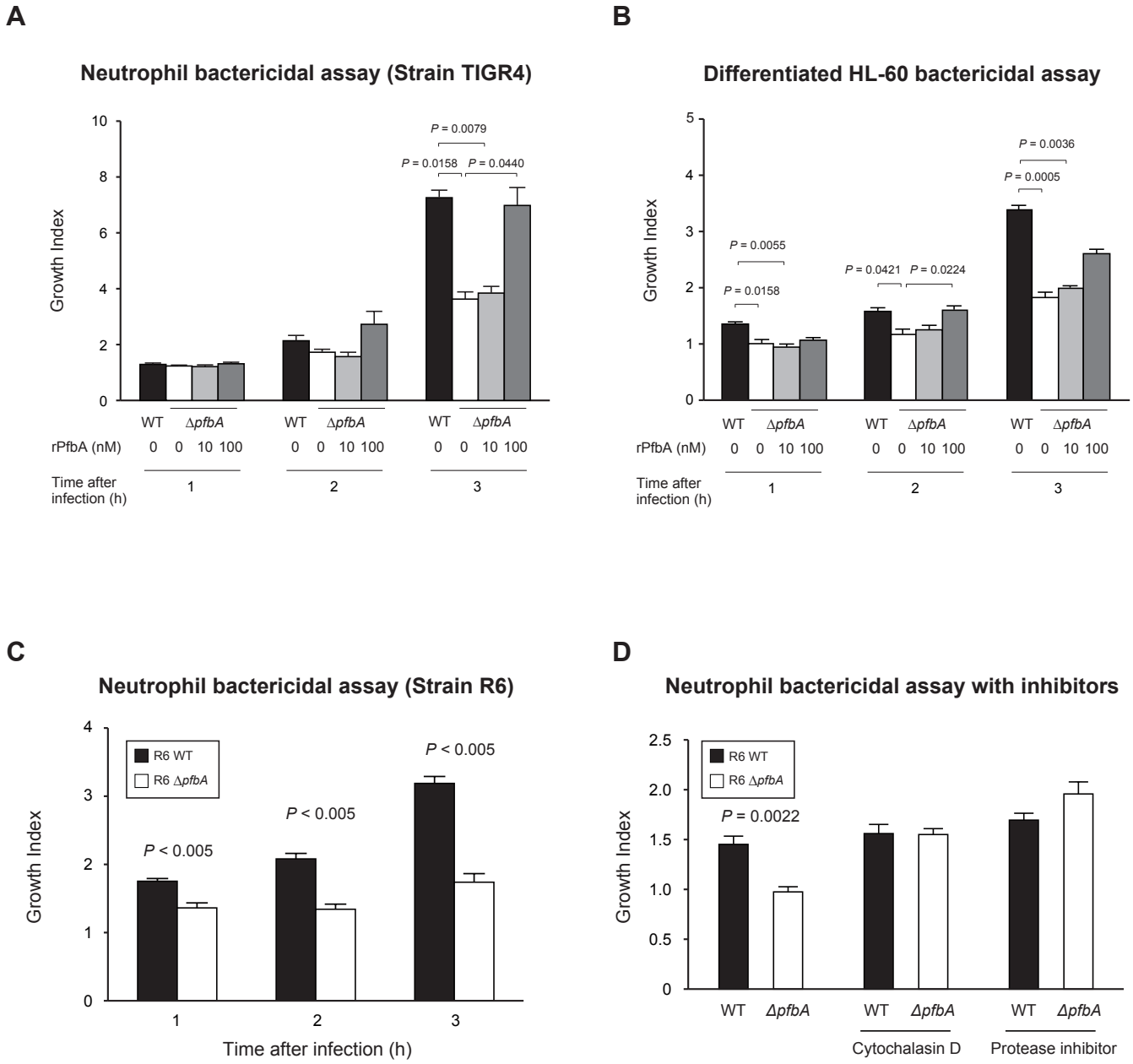

Figure 2. Yamaguchi *et al.*

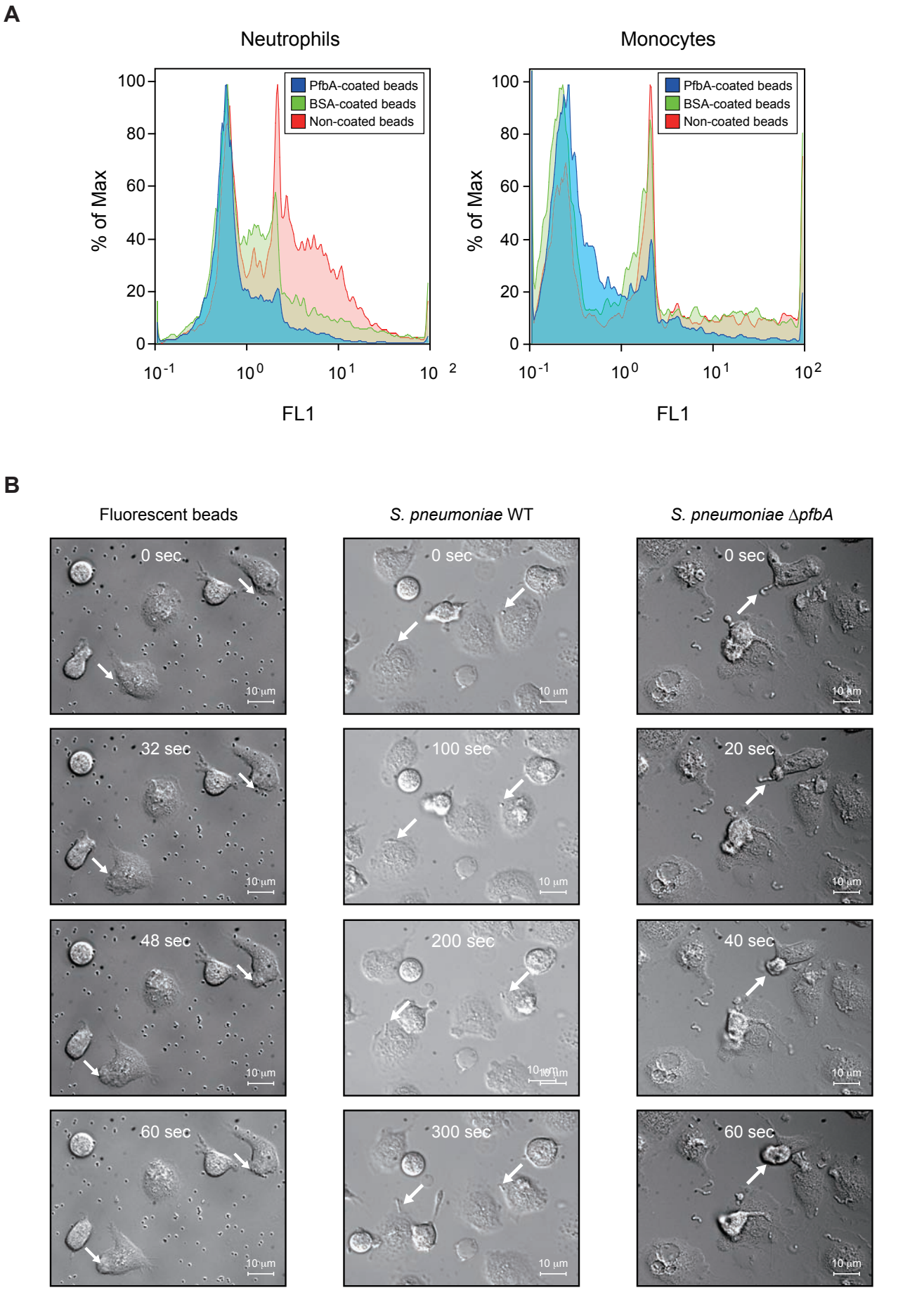

Figure 3. Yamaguchi *et al.*

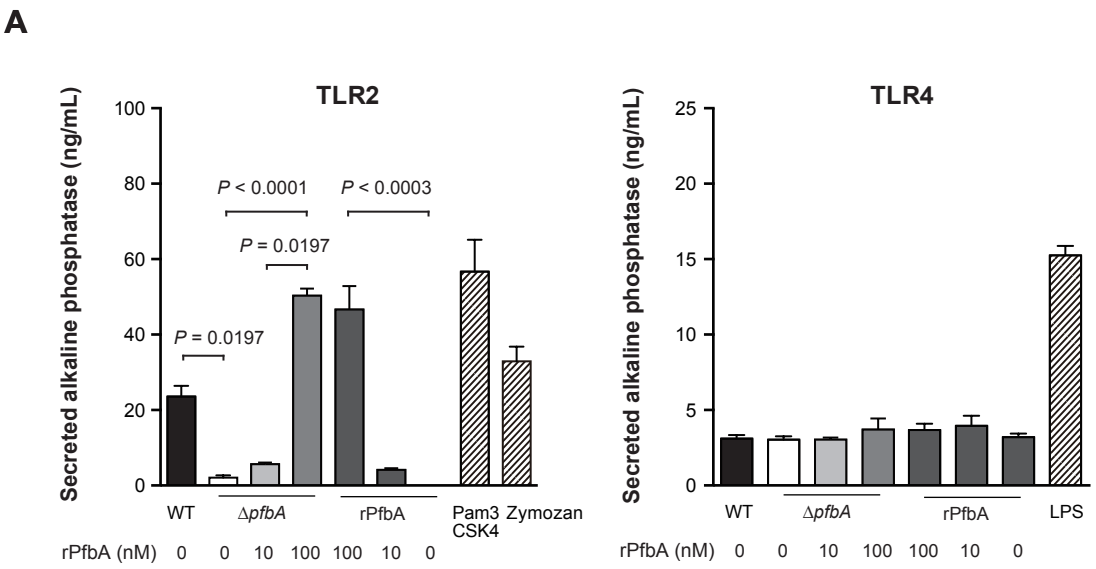

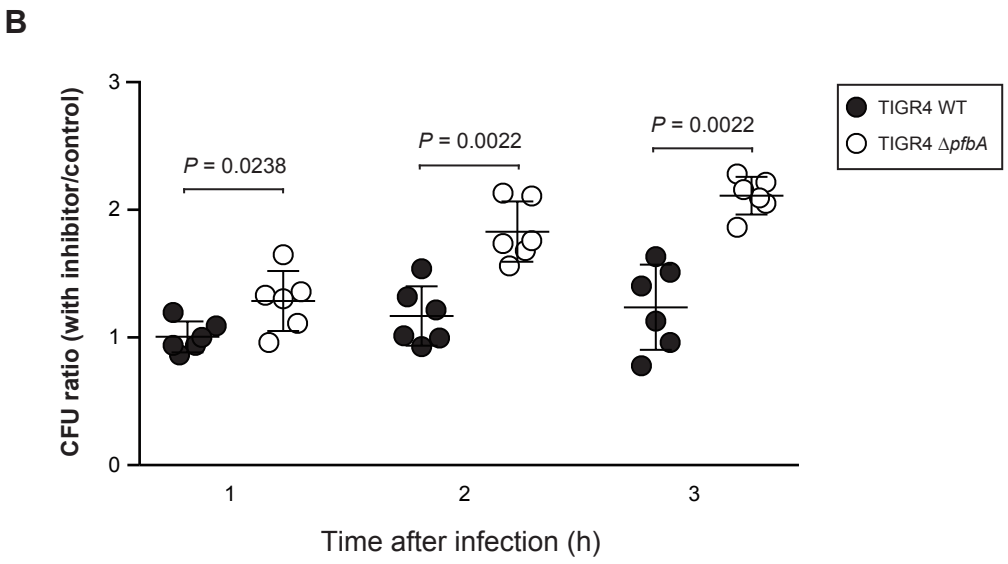

Figure 4. Yamaguchi *et al.*

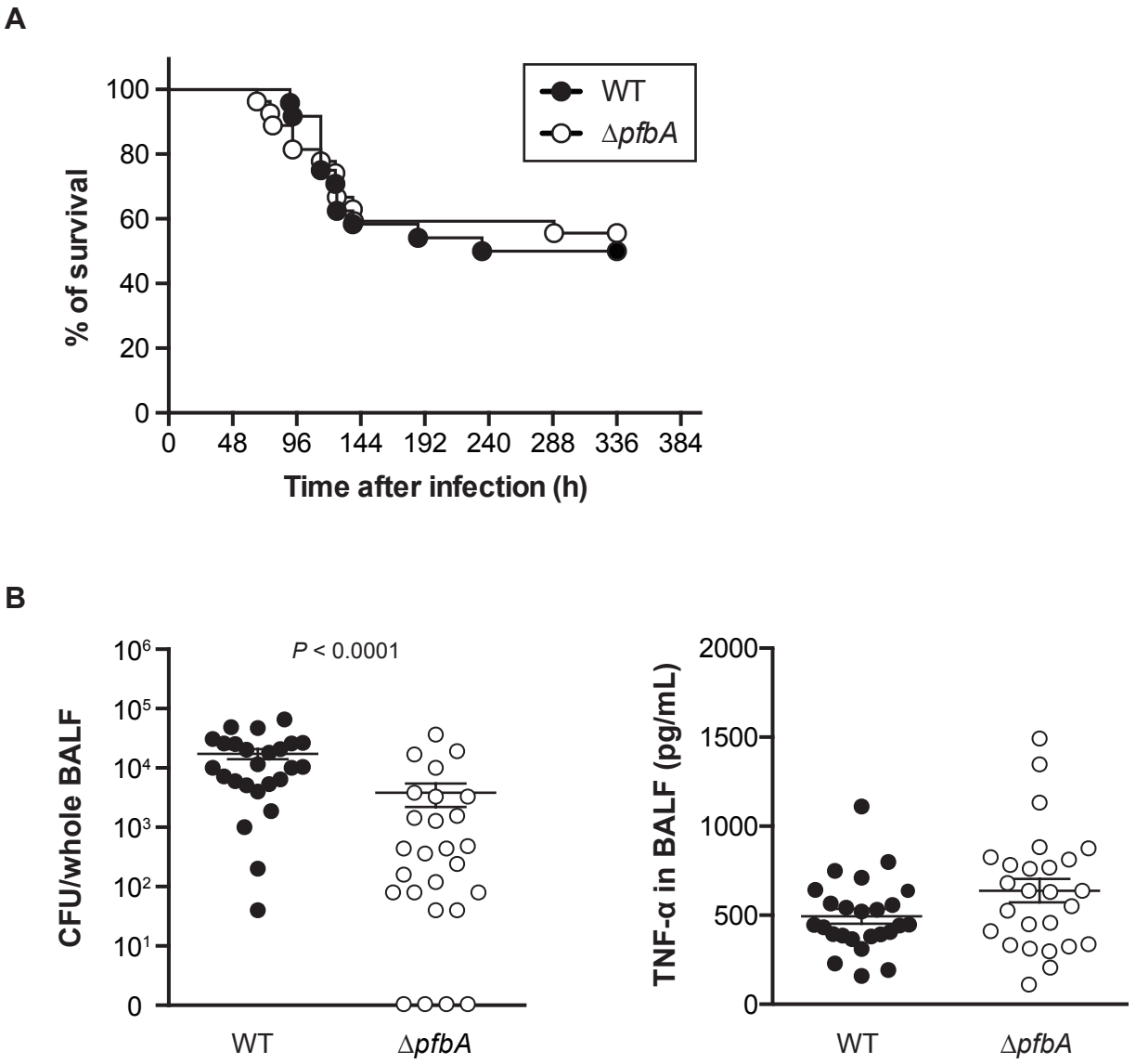

Figure 5. Yamaguchi *et al.*

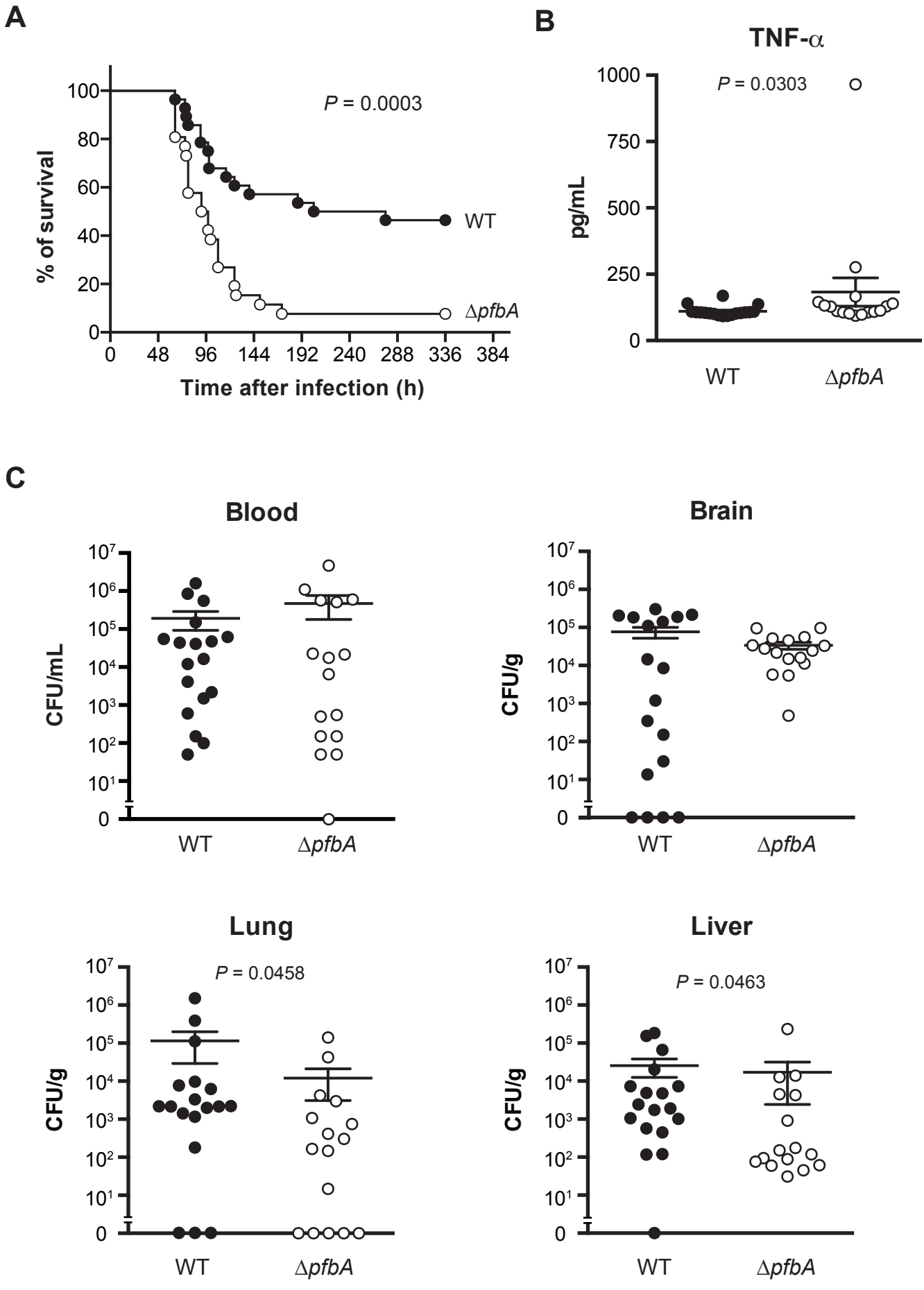

Figure 6. Yamaguchi *et al.*